

# Chemical Reaction in a steady MHD flow with radiation and thermal conductivity over a porous inclined surface

Vibhor Tomer\* Manoj Kumar

Department of Mathematics, Statistics and Computer Science  
G. B. Pant University of Agriculture & Technology, Pantnagar – 263145, Uttarakhand, India

## Abstract

A steady two dimensional mixed convective hydromagnetic flow over an inclined porous surface has been considered. The governing boundary layer equations and boundary conditions are transformed by a scaling group of transformation and finally solved numerically by using Runge-Kutta fourth-fifth order numerical method with shooting technique. Effects of suction/ injection, porosity, thermal radiation, chemical reaction parameter, Schmidt number and Prandtl number on velocity temperature and concentration profile presented graphically and discussed in detail. It is observed that velocity increases while temperature and concentration decreases with increasing values of chemical reaction parameter. The values of physical quantities like skin friction coefficient, Nusselt number and Sherwood number are also tabulated with the variation of physical parameters.

**Keywords:** Chemical reaction, mass transfer, MHD, radiation, porosity, inclined surface

## 1. Introduction

The effects of chemically reactive solute distribution on fluid flow due to a stretching/ shrinking surface have great importance in engineering researches. The chemical reaction effects were studied by many researchers as Chambre and Young (1958) studied the diffusion of a chemically reactive species in a laminar boundary layer flow over a flat plate. The effect of transfer of chemically reactive species in the laminar flow over a stretching sheet examined by Andersson *et al.* (1994). Takhar *et al.* (2000) explicated the flow and mass transfer on a stretching sheet with a magnetic field and chemically reactive species with n-th order reaction. Afify (2004) analyzed the MHD free convective flow of viscous incompressible fluid and mass transfer over a stretching sheet with chemical reaction. Liu (2005) studied the momentum, heat and mass transfer of a hydromagnetic flow past a stretching sheet in the presence of a uniform transverse magnetic field. Akyildiz *et al.* (2006) obtained a solution for diffusion of chemically reactive species in a flow of a non-Newtonian fluid over a stretching sheet immersed in a porous medium. Rahman and Sattar (2006) analyzed the MHD convective flow of a micro polar fluid past a continuously moving vertical porous plate in the presence of heat generation/ absorption. Cortell (2007) studied the motion and mass transfer for two classes of viscoelastic fluid over a porous stretching sheet with chemically reactive species. Raji Reddy and Srihari (2009) studied numerical solution of unsteady flow of a radiating and chemically reacting fluid with time-dependent suction. Kandasamy *et al.* (2010) investigated the effects of temperature-dependent fluid viscosity and chemical reaction on MHD free convective heat and mass transfer with variable stream conditions. Uddin *et al.* (2011) studied the distribution of the chemically reactant solute in the MHD flow of an electrically conducting viscous incompressible fluid over a stretching surface. Hamad *et al.* (2012) studied a steady laminar 2-D MHD viscous incompressible flow over a permeable flat plate with thermal convective boundary condition, radiation effects and similarity representation of the governing partial differential equations obtained by group method. Ferdows *et al.* (2013) investigated a free convective heat and mass transfer flow over a moving permeable flat vertical stretching sheet in the presence of non-uniform magnetic field. Effects of thermal radiation and convective surface boundary condition on steady boundary layer flow of a

viscous incompressible electrically conducting fluid are considered. A scaling group of transformation is applied to the governing equations and the boundary conditions. The objective of present investigation is to study chemical effects on MHD flow over a permeable porous inclined surface. To finding the solution, authors are using scaling group method of transformation. The attempt has also been made to study the effects of radiation, suction/ injection, porosity, thermal radiation, magnetic parameter, radiation parameter, Schmidt number, Prandtl number on the fluid flow and the rate of heat and mass transfer.

## 2. Mathematical Formulation of the Problem

Consider a two dimensional steady laminar flow of an incompressible MHD fluid over an inclined porous flat surface with an acute angle  $\alpha$  to the vertical. With the x-axis measured along the plate, a magnetic field  $B$  is applied in the y-direction that is normal to the flow direction. Suction or injection is imposed on the porous surface. The temperature of the surface is held uniform at  $T_w$  which is higher than the ambient temperature  $T_\infty$ . The species concentration at the surface is maintained uniform at  $C_w = 1$  while the ambient fluid concentration is assumed to be  $C_\infty$ .

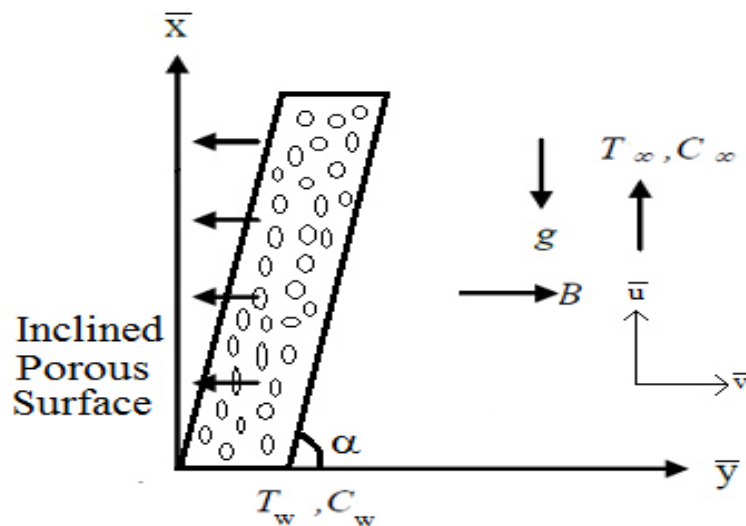


Figure 1. The physical model of the problem

Under these assumptions the governing fluid flow equations of continuity, momentum, heat transfer and mass transfer respectively are as follows:

$$\bar{u} \frac{\partial \bar{u}}{\partial \bar{x}} + \bar{v} \frac{\partial \bar{u}}{\partial \bar{y}} = 0 \quad (1)$$

$$\bar{u} \frac{\partial \bar{u}}{\partial \bar{x}} + \bar{v} \frac{\partial \bar{u}}{\partial \bar{y}} = \left( \nu + \frac{\kappa}{\rho} \right) \frac{\partial^2 \bar{u}}{\partial \bar{y}^2} - \frac{\sigma B^2}{\rho} \bar{u} - \frac{\mu \bar{u}}{\rho K} + g\beta_T (T - T_\infty) \cos \alpha + g\beta_C (C - C_\infty) \cos \alpha \quad (2)$$

$$\bar{u} \frac{\partial T}{\partial \bar{x}} + \bar{v} \frac{\partial T}{\partial \bar{y}} = \frac{k^*}{\rho C_p} \frac{\partial^2 T}{\partial \bar{y}^2} - \frac{1}{\rho C_p} \frac{\partial q_r}{\partial \bar{y}} + \frac{\mu}{\rho C_p} \left( \frac{\partial \bar{u}}{\partial \bar{y}} \right)^2 \quad (3)$$

$$\bar{u} \frac{\partial C}{\partial \bar{x}} + \bar{v} \frac{\partial C}{\partial \bar{y}} = D \frac{\partial^2 C}{\partial \bar{y}^2} - K_c (C - C_\infty) \quad (4)$$

Here  $\bar{u}$  and  $\bar{v}$  are the velocity components in  $\bar{x}$  and  $\bar{y}$  directions, respectively,  $\nu$  is the kinematic coefficient of viscosity,  $\mu$  is coefficient of viscosity,  $\kappa$  is vortex viscosity,  $\sigma$  is electrical conductivity of the fluid,  $K$  is porosity parameter,  $\rho$  is fluid density,  $T$  is fluid temperature,  $\beta_T$  is thermal expansion coefficient,  $\beta_C$  is concentration expansion coefficient,  $k^*$  is the thermal conductivity,  $C_p$  is specific heat,  $D$  is mass diffusivity,  $K_c$  is coefficient of chemical reaction.

The boundary conditions are given by

$$\bar{u} = u_w = c\bar{x}, \bar{v} = -v_w, C = C_w, T = T_w \quad \text{at } \bar{y} = 0 \quad (5a)$$

$$\bar{u} \rightarrow 0, T \rightarrow T_\infty, C \rightarrow C_\infty \quad \text{as } \bar{y} \rightarrow \infty \quad (5b)$$

By using Rosseland's approximation, the radiative heat flux  $q_r$  is given by

$$q_r = -\frac{4\sigma_1}{3k_1} \frac{\partial T^4}{\partial \bar{y}} \quad (6)$$

Here  $\sigma_1$  is the Stefan-Boltzman constant and  $k_1$  is the absorption coefficient. It is assumed that the temperature variation within the flow is such that  $T^4$  may be expanded in a Taylor series about  $T_\infty$  and neglecting higher order terms, we get

$$T^4 \cong 4TT_\infty^3 - 3T_\infty^4 \quad (7)$$

Equations (6) and (7) give

$$\frac{\partial q_r}{\partial \bar{y}} = -\frac{16\sigma_1 T_\infty^3}{3k_1} \frac{\partial^2 T}{\partial \bar{y}^2} \quad (8)$$

Using equations (8) the energy equation (3) becomes

$$\bar{u} \frac{\partial T}{\partial \bar{x}} + \bar{v} \frac{\partial T}{\partial \bar{y}} = \frac{k^*}{\rho C_p} \frac{\partial^2 T}{\partial \bar{y}^2} - \frac{16\sigma_1 T_\infty^3}{3\kappa_1 C_p \rho} \frac{\partial^2 T}{\partial \bar{y}^2} + \frac{\mu}{\rho C_p} \left( \frac{\partial \bar{u}}{\partial \bar{y}} \right)^2 \quad (9)$$

Introducing the following dimensionless variables as considered by Hamad et al. (2012):

$$x = \frac{\bar{x}}{L}, \quad y = \frac{\bar{y}\sqrt{Re}}{L}, \quad u = \frac{\bar{u}}{u_\infty}, \quad \bar{v} = \frac{v\sqrt{Re}}{u_\infty}, \quad \theta = \frac{T - T_\infty}{T_f - T_\infty}, \quad \phi = \frac{C - C_\infty}{C_w - C_\infty} \quad (10a)$$

$$u = \frac{\partial \psi}{\partial y}, \quad v = -\frac{\partial \psi}{\partial x} \quad (10b)$$

where  $Re = u_\infty L/\nu$  is the Reynolds number,  $\psi$  is the stream function,  $L$  being the characteristic length and  $u_\infty$  is reference velocity.

Hence, equations (2), (9) and (4) reduce in the following form:

$$\frac{\partial \psi}{\partial y} \frac{\partial^2 \psi}{\partial x \partial y} - \frac{\partial \psi}{\partial x} \frac{\partial^2 \psi}{\partial y^2} - (1 + K) \frac{\partial^3 \psi}{\partial y^3} + (M + K_p) \frac{\partial \psi}{\partial y} - \frac{\cos \alpha}{Re^2} (Gr\theta + \phi Gc) = 0 \quad (11)$$

$$\frac{\partial \psi}{\partial y} \frac{\partial \theta}{\partial x} - \frac{\partial \psi}{\partial x} \frac{\partial \theta}{\partial y} - \frac{1}{Pr} \frac{\partial^2 \theta}{\partial y^2} - \frac{4}{3} \frac{1}{RPr} \frac{\partial^2 \theta}{\partial y^2} - Ec \left( \frac{\partial^2 \psi}{\partial y^2} \right)^2 = 0 \quad (12)$$

$$\frac{\partial \psi}{\partial y} \frac{\partial \phi}{\partial x} - \frac{\partial \psi}{\partial x} \frac{\partial \phi}{\partial y} - \frac{1}{Sc} \frac{\partial^2 \phi}{\partial y^2} + \gamma \phi = 0 \quad (13)$$

Subject to boundary conditions,

$$\frac{\partial \psi}{\partial y} = x, \quad \frac{\partial \psi}{\partial x} = -\frac{v_w}{u_\infty \sqrt{Re}}, \quad \theta = 1, \quad \phi = 1 \quad \text{at } y = 0 \quad (14a)$$

$$\frac{\partial \psi}{\partial y} \rightarrow 0, \quad \theta \rightarrow 0, \quad \phi \rightarrow 0 \quad \text{as } y \rightarrow \infty \quad (14a)$$

where  $K = \frac{\kappa}{\mu}$  is material parameter,  $M = \frac{\sigma B^2 L}{\rho u_\infty}$  is the Hartmann number,  $K_p = \frac{L \mu}{U_\infty \rho K'}$  is the porosity parameter,

$Gr = \frac{gL^3 \beta_T (T_w - T_\infty)}{v^2}$  and  $Gc = \frac{gL^3 \beta_C (C_w - C_\infty)}{v^2}$  are thermal and mass Grashof number respectively,

$R = \frac{k_1 k^*}{4T_\infty^3 \sigma}$  is the conduction-radiation parameter,  $Pr = \frac{\mu C_p}{k^*}$  is the Prandtl number,  $Ec = \frac{U_\infty^2}{C_p (T_w - T_\infty)}$  is the

Eckert number,  $Sc = \frac{v}{D}$  is the Schmidt number,  $\gamma = \frac{K_c L}{U_\infty}$  is the chemical reaction rate parameter.

The application of group transformations has been considered to find similarity reduction of equations (11), (12) and (13). Consider the following group transformations

$$\Gamma : x^\# = x \Omega^{\alpha_1}, \quad y^\# = y \Omega^{\alpha_2}, \quad \psi^\# = \psi \Omega^{\alpha_3}, \quad \theta^\# = \theta \Omega^{\alpha_4}, \quad \phi^\# = \phi \Omega^{\alpha_5} \quad (15)$$

where  $\alpha_1, \alpha_2, \alpha_3, \alpha_4$  and  $\alpha_5$  are constants and  $\Omega$  is the parameter of point transformation. Now finding the relation among  $\alpha$ 's such that

$$\Delta_j(x^\#, y^\#, \psi^\#, \theta^\#, \phi^\#, \dots, \frac{\partial^3 \psi^\#}{\partial y^{\#3}}) = H_j(x, y, \psi, \theta, \phi, \dots, \frac{\partial^3 \psi}{\partial y^3}) \varphi_j(x, y, \psi, \theta, \phi, \dots, \frac{\partial^3 \psi}{\partial y^3}) \quad (j=1,2,3) \quad \Delta_1,$$

$\Delta_2$  and  $\Delta_3$  are conformally invariant under the group transformation (15).

By using above group transformation in equation (11) and solving the resulting equations one finds the following

$$\alpha_2 = \alpha_4 = \alpha_5 = 0 \quad \text{and} \quad \alpha_1 = 2\alpha_3 \quad (16)$$

Similarly equations (12), (13) and (14) are also giving  $\alpha_1 = 2\alpha_3, \alpha_2 = \alpha_4 = \alpha_5 = 0$ , so these equations show invariant under the group transformation (15).

Now the characteristic equations are

$$\frac{dx}{2x} = \frac{dy}{0} = \frac{d\psi}{\psi} = \frac{d\theta}{0} = \frac{d\phi}{0} \quad (17)$$

which give the following similarity transformations:

$$\eta = y, \quad \psi = x^{\frac{1}{2}} f(\eta), \quad \theta = \theta(\eta), \quad \text{and} \quad \phi = \phi(\eta) \quad (18)$$

Using these transformations, the momentum, energy and mass equations become

$$f''' = \frac{1}{1+K} \left[ 0.5(f'^2 - ff'') + (M + K_p)f' - \frac{\cos\alpha}{Re^2} (Gr\theta + \phi Gc) \right] \quad (19)$$

$$\theta'' = \frac{-1}{3R + 4} (1.5RPrf'\theta' + 3RPrEc f''^2) \quad (20)$$

$$\phi'' = Sc(\phi\gamma - 0.5f\phi') \quad (21)$$

Subject to the boundary conditions

$$f = f_w, f' = 1, \theta = 1, \phi = 1 \quad \text{at} \quad \eta = 0 \quad (22b)$$

$$f' \rightarrow 0, \theta \rightarrow 0, \phi \rightarrow 0 \quad \text{as} \quad \eta \rightarrow \infty \quad (22b)$$

The physical quantities of interest are the Skin friction coefficient  $C_f$ , Nusselt number  $Nu$  and Sherwood number  $Sh$ , which are defined as

$$C_f = \frac{\mu}{\rho \bar{u}^2} \left( \frac{\partial \bar{u}}{\partial \bar{y}} \right)_{\bar{y}=0}, \quad Nu = \frac{-\bar{x}}{T_f - T_\infty} \left( \frac{\partial T}{\partial \bar{y}} \right)_{\bar{y}=0}, \quad Sh = \frac{-\bar{x}}{C_w - C_\infty} \left( \frac{\partial C}{\partial \bar{y}} \right)_{\bar{y}=0} \quad (23)$$

### 3. Method of solution

The system of ordinary differential equations (19), (20) and (21) subject to the boundary conditions (22) have been solved numerically using Runge-Kutta method with shooting technique. The computations were carried out using step size of  $\Delta\eta = 0.01$  selected to be satisfactory for a convergence criterion of  $10^{-6}$  in all cases.

The physical quantities skin friction coefficient  $C_f$ , Nusselt number  $Nu$  and Sherwood number  $Sh$  indicate the wall shear stress, rate of heat transfer and rate of mass transfer respectively and these are proportional to the numerical values of  $f''(0)$ ,  $-\theta'(0)$  and  $-\phi'(0)$  respectively.

### 4. Results and discussion

The numerical results for velocity, temperature, concentration, wall heat transfer, the rate of heat and mass transfer have been computed and represented. The computations are carried out for different values of different parameters. The calculations were made by taking material parameter  $k$  ( $= 0.1, 0.2, 0.5$ ), porosity parameter  $K_p$  ( $= 0.1, 0.4, 0.7$ ), chemical reaction parameter ( $0.1 \leq \gamma \leq 1$ ), radiation parameter ( $0.2 \leq R \leq 1$ ),  $0^\circ \leq \alpha \leq 50^\circ$   $Sc = (0.22, 0.72, 6.8, 10)$  with  $Gr = 0.1$ ,  $Gc = 0.1$ ,  $Ec = 1$ ,  $Re = 1$  and Prandtl number  $Pr = 0.72$  for air at 1 atmospheric pressure. Different values of magnetic parameter, i.e.  $0.1 \leq M \leq 1$  were taken to analyse the study.

The values for the skin friction coefficient, Nusselt number and Sherwood number have been tabulated in table 1. It is seen that the value of skin friction coefficient varies and is greater for suction while smaller for injection. Nusselt number is less for suction in comparison to injection and Sherwood number is higher for suction while smaller for injection. Figures 2–4 exhibit the effects of magnetic parameter on velocity, temperature and concentration. It is seen that the velocity increases while temperature and concentration decrease with an increase in magnetic parameter. Figures 5–7 show the effect of porosity parameter on velocity, temperature and concentration profile. Velocity first increases then sharply decreases while temperature and concentration decrease increases as the value of  $K_p$ . Figures 8, 9 and 10 depict the effect of inclined plate angle  $\alpha$  on different profiles and it has been seen that velocity increases with its increasing values (for  $\alpha = 0^\circ, 30^\circ, 50^\circ$ ), while temperature and concentration decrease with its increase. Figures 11, 12 and 13 show the variation of velocity,

temperature and concentration respectively for the variation of radiation parameter R. It is observed that velocity and temperature decrease while concentration increases with an increase in radiation parameter. Figures 14–16 show the effect of chemical reaction parameter  $\gamma$  on velocity, temperature and concentration. Velocity increases while temperature and concentration decrease as the value of  $\gamma$  increases. The effect of Schmidt number Sc on concentration is represented through figure 17. It has been observed that concentration decreases as Schmidt number increases. The effect of Prandtl number Pr on velocity and temperature are represented by figures 18 and 19 respectively. It is observed that the velocity first increases then sharply decreases while temperature decrease with its increasing values (for Pr = 0.22, 6.8, 10).

**Table 1.** Effect on Skin friction coefficient  $C_f$ , Nusselt number Nu and Sherwood number Sh for  $f_w = 0.5$ ,  $K = 0.1$ ,  $K_p = 0.1$ ,  $M = 0.5$ ,  $Sc = 0.5$ ,  $Pr = 0.72$ ,  $R = 1$ ,  $Re = 1$ ,  $Gr = 0.1$ ,  $Gc = 0.1$ ,  $Ec = 1$ ,  $\alpha = 30^\circ$  and  $\gamma = 0.1$ .

parameter	values	$f''(0)$	$\theta'(0)$	$\phi'(0)$
$\gamma$	0.1	0.000014	-0.295051	-0.507571
	0.5	0.001001	-0.298502	-0.689439
	1	0.015202	-0.306302	-0.863251
$K_p$	0.1	0.000014	-0.295051	-0.507571
	0.4	0.352910	-0.286591	-0.530115
	0.7	0.838471	-0.241011	-0.563746
M	0.1	-0.452104	-0.218399	-0.464637
	0.5	0.000014	-0.295051	-0.507571
	1	0.659101	-0.334052	-0.551361
$\alpha$	$0^\circ$	0.000014	-0.286051	-0.504839
	$30^\circ$	0.000014	-0.295051	-0.507571
	$50^\circ$	0.001020	-0.309251	-0.511870
R	0.2	0.097521	-0.149050	-0.522674
	0.5	0.047521	-0.231590	-0.515161
	1	0.000014	-0.295051	-0.507571
Pr	0.22	0.075901	-0.143201	-0.519201
	6.8	0.010013	-1.327659	-0.511292
	10	0.001004	-1.746591	-0.510820

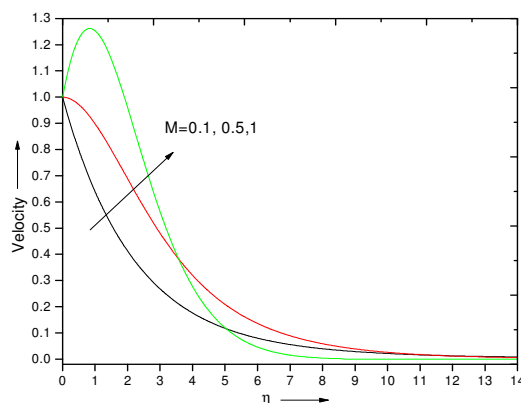


Figure 2. Effect of magnetic parameter M on velocity  $f'$  for  $f_w = 0.5$ ,  $K = 0.1$ ,  $K_p = 0.1$ ,  $Sc = 0.5$ ,  $Pr = 0.72$ ,  $R = 1$ ,  $Re = 1$ ,  $Gr = 0.1$ ,  $Gc = 0.1$ ,  $Ec = 1$ ,  $\alpha = 30^\circ$  and  $\gamma = 0.1$ .

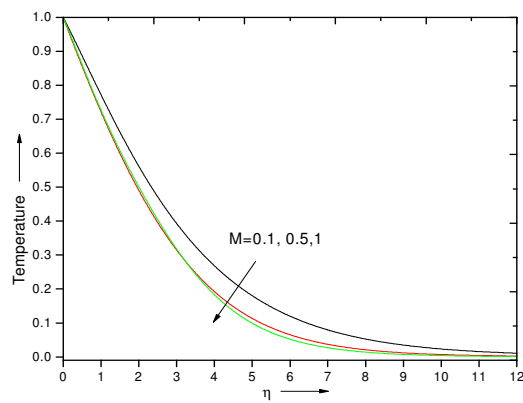


Figure 3. Effect of magnetic parameter  $M$  on temperature  $\theta$  for  $f_w = 0.5$ ,  $K = 0.1$ ,  $K_p = 0.1$ ,  $Sc = 0.5$ ,  $Pr = 0.72$ ,  $R = 1$ ,  $Re = 1$ ,  $Gr = 0.1$ ,  $Gc = 0.1$ ,  $Ec = 1$ ,  $\alpha = 30^\circ$  and  $\gamma = 0.1$ .

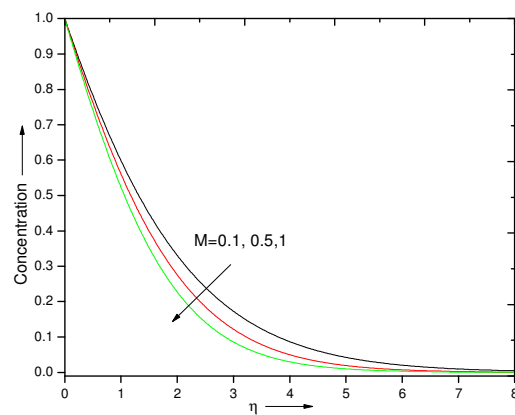


Figure 4. Effect of magnetic parameter  $M$  on concentration  $\phi$  for  $f_w = 0.5$ ,  $K = 0.1$ ,  $K_p = 0.1$ ,  $Sc = 0.5$ ,  $Pr = 0.72$ ,  $R = 1$ ,  $Re = 1$ ,  $Gr = 0.1$ ,  $Gc = 0.1$ ,  $Ec = 1$ ,  $\alpha = 30^\circ$  and  $\gamma = 0.1$ .

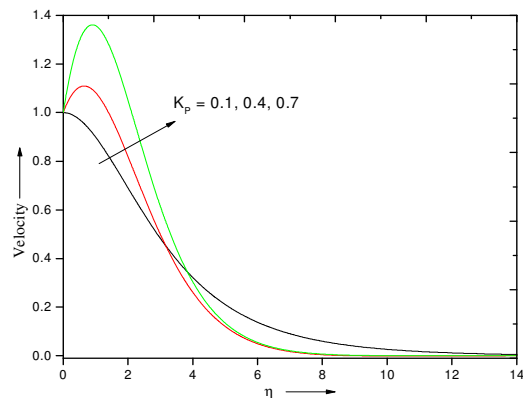


Figure 5. Effect of porosity parameter  $K_p$  on velocity  $f'$  for  $f_w = 0.5$ ,  $K = 0.1$ ,  $M = 0.5$ ,  $Sc = 0.5$ ,  $Pr = 0.72$ ,  $R = 1$ ,  $Re = 1$ ,  $Gr = 0.1$ ,  $Gc = 0.1$ ,  $Ec = 1$ ,  $\alpha = 30^\circ$  and  $\gamma = 0.1$ .

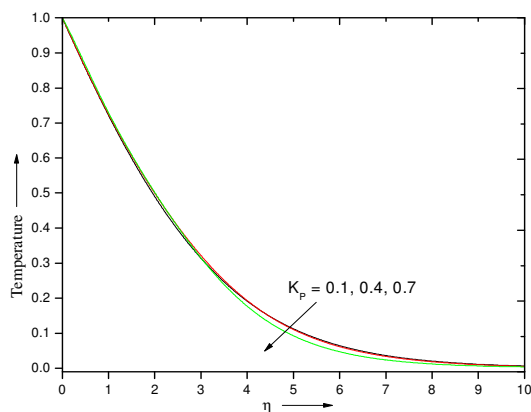


Figure 6. Effect of porosity parameter  $K_p$  on temperature  $\theta$  for  $f_w = 0.5$ ,  $K = 0.1$ ,  $M = 0.5$ ,  $Sc = 0.5$ ,  $Pr = 0.72$ ,  $R = 1$ ,  $Re = 1$ ,  $Gr = 0.1$ ,  $Gc = 0.1$ ,  $Ec = 1$ ,  $\alpha = 30^\circ$  and  $\gamma = 0.1$ .

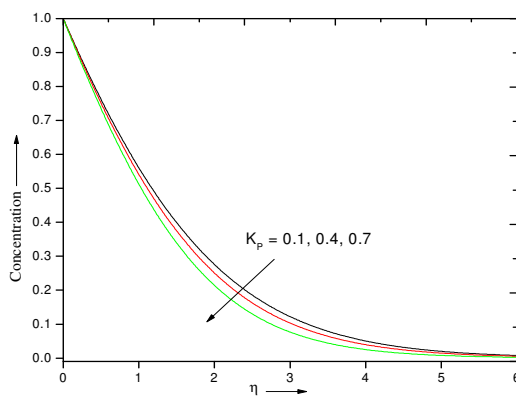


Figure 7. Effect of porosity parameter  $K_p$  on concentration  $\phi$  for  $f_w = 0.5$ ,  $K = 0.1$ ,  $M = 0.5$ ,  $Sc = 0.5$ ,  $Pr = 0.72$ ,  $R = 1$ ,  $Re = 1$ ,  $Gr = 0.1$ ,  $Gc = 0.1$ ,  $Ec = 1$ ,  $\alpha = 30^\circ$  and  $\gamma = 0.1$ .

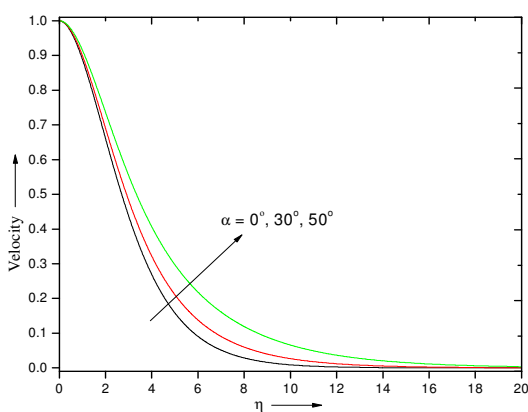


Figure 8. Effect of  $\alpha$  on velocity  $f'$  for  $f_w = 0.5$ ,  $K = 0.1$ ,  $K_p = 0.1$ ,  $M = 0.5$ ,  $Sc = 0.5$ ,  $Pr = 0.72$ ,  $R = 1$ ,  $Re = 1$ ,  $Gr = 0.1$ ,  $Gc = 0.1$ ,  $Ec = 1$  and  $\gamma = 0.1$ .



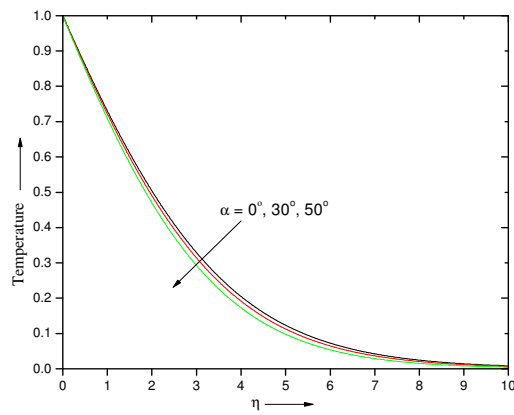


Figure 9. Effect of  $\alpha$  on temperature  $\theta$  for  $f_w = 0.5$ ,  $K = 0.1$ ,  $K_p = 0.1$ ,  $M = 0.5$ ,  $Sc = 0.5$ ,  $Pr = 0.72$ ,  $R = 1$ ,  $Re = 1$ ,  $Gr = 0.1$ ,  $Gc = 0.1$ ,  $Ec = 1$  and  $\gamma = 0.1$ .

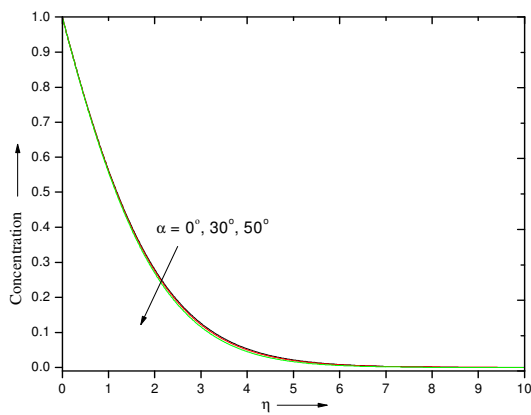


Figure 10. Effect of  $\alpha$  on concentration  $\phi$  for  $f_w = 0.5$ ,  $K = 0.1$ ,  $K_p = 0.1$ ,  $M = 0.5$ ,  $Sc = 0.5$ ,  $Pr = 0.72$ ,  $R = 1$ ,  $Re = 1$ ,  $Gr = 0.1$ ,  $Gc = 0.1$ ,  $Ec = 1$  and  $\gamma = 0.1$ .

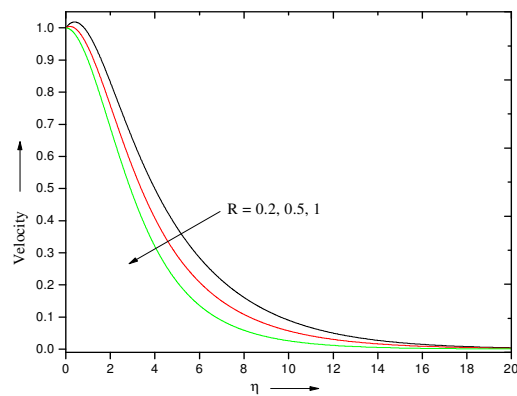


Figure 11. Effect of radiation parameter  $R$  on velocity  $f'$  for  $f_w = 0.5$ ,  $K = 0.1$ ,  $K_p = 0.1$ ,  $M = 0.5$ ,  $Sc = 0.5$ ,  $Pr = 0.72$ ,  $Re = 1$ ,  $Gr = 0.1$ ,  $Gc = 0.1$ ,  $Ec = 1$ ,  $\alpha = 30^\circ$  and  $\gamma = 0.1$ .

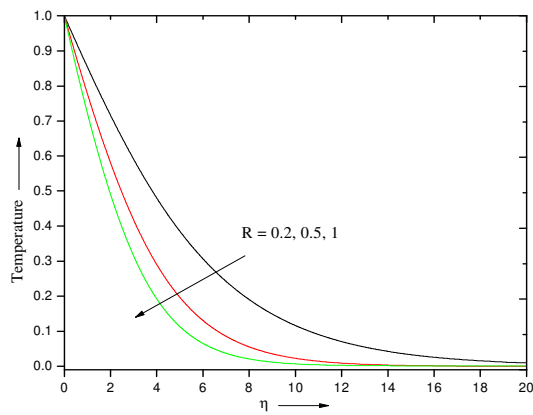


Figure 12. Effect of radiation parameter  $R$  on temperature  $\theta$  for  $f_w = 0.5$ ,  $K = 0.1$ ,  $K_p = 0.1$ ,  $M = 0.5$ ,  $Sc = 0.5$ ,  $Pr = 0.72$ ,  $Re = 1$ ,  $Gr = 0.1$ ,  $Gc = 0.1$ ,  $Ec = 1$ ,  $\alpha = 30^\circ$  and  $\gamma = 0.1$ .

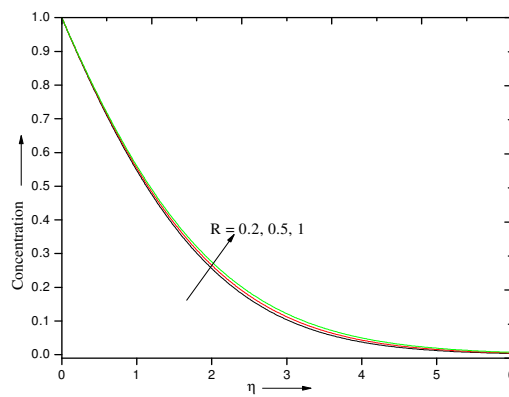


Figure 13. Effect of radiation parameter  $R$  on concentration  $\phi$  for  $f_w = 0.5$ ,  $K = 0.1$ ,  $K_p = 0.1$ ,  $M = 0.5$ ,  $Sc = 0.5$ ,  $Pr = 0.72$ ,  $Re = 1$ ,  $Gr = 0.1$ ,  $Gc = 0.1$ ,  $Ec = 1$ ,  $\alpha = 30^\circ$  and  $\gamma = 0.1$ .

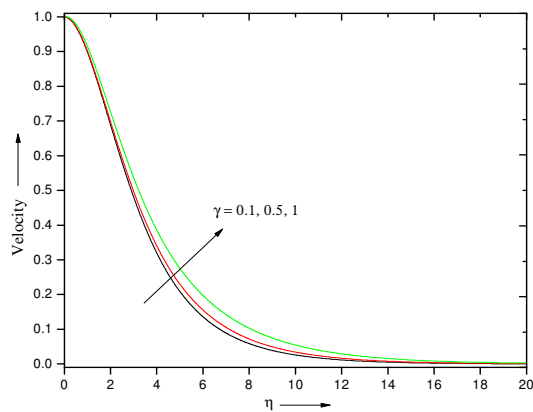


Figure 14. Effect of chemical reaction parameter  $\gamma$  on velocity  $f'$  for  $f_w = 0.5$ ,  $K = 0.1$ ,  $K_p = 0.1$ ,  $M = 0.5$ ,  $Sc = 0.5$ ,  $Pr = 0.72$ ,  $R = 1$ ,  $Re = 1$ ,  $Gr = 0.1$ ,  $Gc = 0.1$ ,  $Ec = 1$  and  $\alpha = 30^\circ$ .

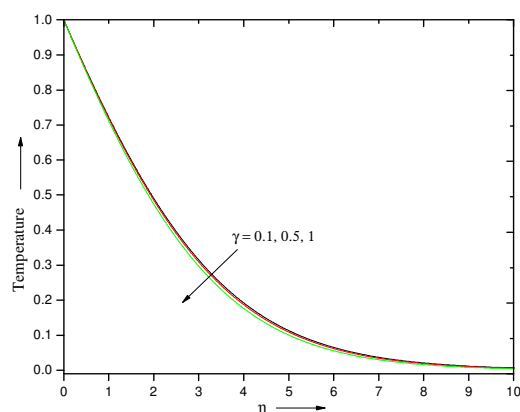


Figure 15. Effect of chemical reaction parameter  $\gamma$  on temperature  $\theta$  for  $f_w = 0.5$ ,  $K = 0.1$ ,  $K_p = 0.1$ ,  $M = 0.5$ ,  $Sc = 0.5$ ,  $Pr = 0.72$ ,  $R = 1$ ,  $Re = 1$ ,  $Gr = 0.1$ ,  $Gc = 0.1$ ,  $Ec = 1$  and  $\alpha = 30^\circ$ .

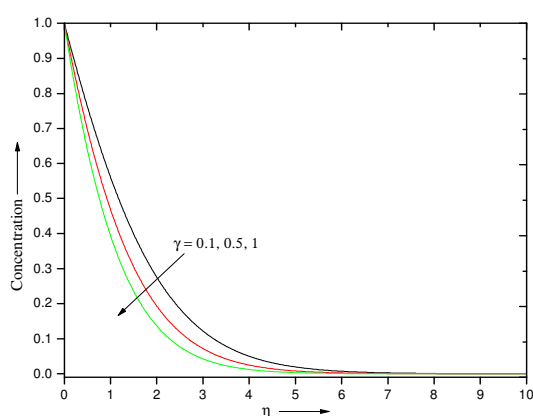


Figure 16. Effect of chemical reaction parameter  $\gamma$  on concentration  $\phi$  for  $f_w = 0.5$ ,  $K = 0.1$ ,  $K_p = 0.1$ ,  $M = 0.5$ ,  $Sc = 0.5$ ,  $Pr = 0.72$ ,  $R = 1$ ,  $Re = 1$ ,  $Gr = 0.1$ ,  $Gc = 0.1$ ,  $Ec = 1$  and  $\alpha = 30^\circ$ .

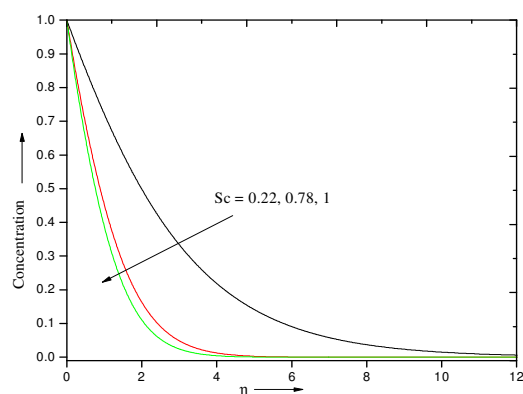


Figure 17. Effect of Schmidt number  $Sc$  on concentration  $\phi$  for  $f_w = 0.5$ ,  $K = 0.1$ ,  $K_p = 0.1$ ,  $M = 0.5$ ,  $Pr = 0.72$ ,  $R = 1$ ,  $Re = 1$ ,  $Gr = 0.1$ ,  $Gc = 0.1$ ,  $Ec = 1$ ,  $\alpha = 30^\circ$  and  $\gamma = 0.1$ .

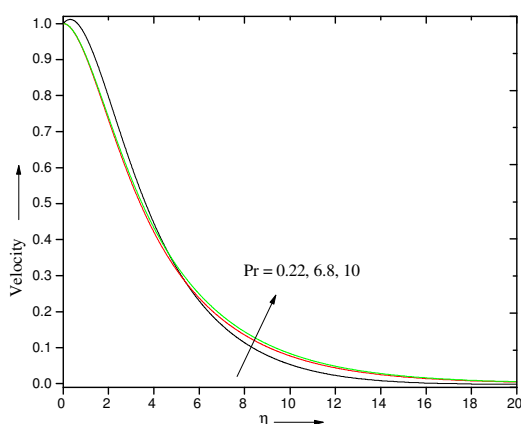


Figure 18. Effect of Prandtl number  $Pr$  on velocity  $f'$  for  $f_w = 0.5$ ,  $K = 0.1$ ,  $K_p = 0.1$ ,  $M = 0.5$ ,  $Sc = 0.5$ ,  $R = 1$ ,  $Re = 1$ ,  $Gr = 0.1$ ,  $Gc = 0.1$ ,  $Ec = 1$ ,  $\alpha = 30^\circ$  and  $\gamma = 0.1$ .

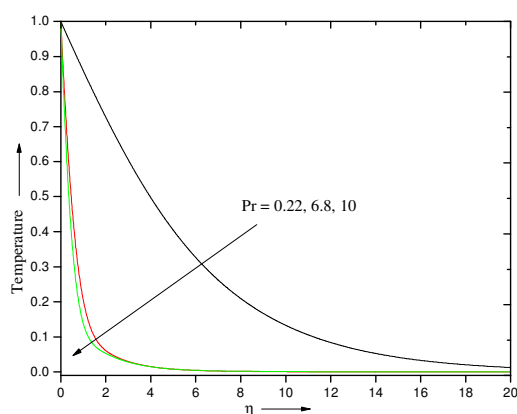


Figure 19. Effect of Prandtl number  $Pr$  on concentration  $\phi$  for  $f_w = 0.5$ ,  $K = 0.1$ ,  $K_p = 0.1$ ,  $M = 0.5$ ,  $Sc = 0.5$ ,  $R = 1$ ,  $Re = 1$ ,  $Gr = 0.1$ ,  $Gc = 0.1$ ,  $Ec = 1$ ,  $\alpha = 30^\circ$  and  $\gamma = 0.1$ .

## References

- Afify, A., (2004), "MHD free convective flow and mass transfer over a stretching sheet with chemical reaction", *Heat and Mass Transfer*. **40**, 495–500.
- Akyildiz, F.T., Bellout, H., Vajravelu, K., (2006), "Diffusion of chemically reactive species in a porous medium over a stretching sheet", *Journal of Mathematical Analysis and Application*. **320**, 322–339.
- Andersson, H.I., Hansen, O.R., Holmedal, B., (1994), "Diffusion of a chemically reactive species from a stretching sheet", *International Journal of Heat and Mass Transfer*. **37**, 659–664.
- Chambre, P.L. and Young, J.D., (1958), "On diffusion of a chemically reactive species in a laminar boundary layer flow", *Physics of Fluids*. **1**, 48–54.
- Chamkha, A.J., (2000), "Thermal radiation and buoyancy effects on hydromagnetic flow over an accelerating permeable surface with heat source or sink", *International Journal of Engineering Science*. **38**, 1699–1712.
- Cortell, R., (2007), "Toward an understanding of the motion and mass transfer with chemically reactive species for two classes of viscoelastic fluid over a porous stretching sheet", *Chemical Engineering and Processing*. **46**, 982–989.
- Ferdows, M., Uddin, M. J., Afify, A.A., (2013), "Scaling group transformation for MHD boundary layer free convective heat and mass transfer flow past a convectively heated nonlinear radiating stretching sheet", *International Journal of Heat and Mass Transfer*. **56**, 181–187.
- Hamad, M.A.A., Uddin, M. J., Ismail, A.I.M., (2012), "Radiation effects on heat and mass transfer in MHD stagnation-point flow over a permeable flat plate with thermal convective surface boundary condition, temperature dependent viscosity and thermal conductivity", *Nuclear Engineering and Design*. **242**, 194–200.

Hayata, T., Shehzad, S.A., Qasim, M., Obaidat, S., (2012), "Radiative flow of Jeffery fluid in a porous medium with power law heat flux and heat source", *Nuclear Engineering and Design*. **243**, 15–19.

Kandasamy, R., Ismoen, M., Saim, H.B., (2010), "Lie group analysis for the effects of temperature-dependent fluid viscosity and chemical reaction on MHD free convective heat and mass transfer with variable stream conditions", *Nuclear Engineering and Design*. **240**, 39–46.

Liu, I-C., (2005), "A note on heat and mass transfer for a hydromagnetic flow over a stretching sheet", *International Communications in Heat and Mass Transfer*. **32**, 1075–1084.

Rahman, M.M. and Sattar, M.A., (2006), "MHD convective flow of a micro polar fluid past a continuously moving vertical porous plate in the presence of heat generation/ absorption", *ASME Journal of Heat Transfer*. **128**, 142–152.

Raji Reddy, S. and Srihari, K., (2009), "Numerical solution of unsteady flow of a radiating and chemically reacting fluid with time-dependent suction", *Indian Journal of Pure and Applied physics*. **47**, 7–11.

Takhar, H.S., Chamkha, A.J., Nath, G., (2000), "Flow and mass transfer on a stretching sheet with a magnetic field and chemically reactive species", *International Journal of Engineering Science*. **38**, 1303–1314.

Uddin, M.S., Bhattacharyya, K., Layek, G.C., Pk, W.A., (2011), "Chemically Reactive Solute Distribution in a Steady MHD Boundary Layer Flow over a Stretching Surface", *JAFM*. **4**, 53–58.

Veerraju, N., Srinivasa Babu, K.S. and Rao, C.N.B., (2012), Mixed Convection at a Vertical Plate in a Porous Medium with Magnetic Field and Variable Viscosity, *JAFM*. **5(4)**, 53–62.